Cement and Concrete Research 40 (2010) 1175–1188

Contents lists available at ScienceDirect

Cement and Concrete Research

journal homepage: http://ees.elsevier.com/CEMCON/default.asp

Accelerated degradation method for cement under CO_2-rich environment: The LIFTCO$_2$ procedure (leaching induced by forced transport in CO_2 fluids)

Gaëtan Rimmelé, Véronique Barlet-Gouédard *

Schlumberger Riboud Product Center, Well Integrity Technologies, 1 rue Henri Becquerel, BP 202, 92142, Clamart, France

ARTICLE INFO

Article history:
Received 24 September 2008
Accepted 19 March 2010

Keywords:
Accelerated degradation tests
Portland cement
Voltage
Forced transport
CO_2 storage

ABSTRACT

For emerging applications such as long-term CO_2 storage, establishing and maintaining well integrity during the life of the well pose significant challenges. Particularly, well cement will need to be durable under corrosive environments, such as exposure to CO_2-rich fluids, over a long period of time from 25 years to 100–1000 years. To model long-term cement durability in such severe environments, accelerated degradation methods must be considered and developed. This study presents experimental equipment and a procedure showing that it is possible to accelerate Portland cement degradation in the presence of CO_2 fluids by applying a potential gradient through a set cement sample in a CO_2 environment (the LIFTCO$_2$ procedure). The degradation pattern consists of a series of successive fronts penetrating the cement sample: a dissolution front, a carbonation front, and a gel layer. Such degradation is accelerated when increasing the potential gradient, the temperature, and the CO_2 concentration in the electrolyte.

1. Introduction

Today, significant challenges for establishing and maintaining well integrity during the life of a well are posed by new emerging applications, such as long-term CO_2 storage. For this application, one must consider the corrosive fluids (CO_2-rich fluids) in the presence of which cement will need to be durable over a long period of time, from 25 years to 100–1000 years. In the last few years, much effort has been devoted to studying the behavior of cement for CO_2 storage. In the laboratory, more and more studies are being done on the integrity of well cements in CO_2-rich environments, in simulating downhole conditions with CO_2-rich fluids and exposing cement to this aggressive environment [1–8]. Depending on the conditions of exposure (e.g. pressure, temperature, CO_2 + water vs. CO_2 + brine), these studies highlight different degrees of cement degradation due to the CO_2 fluids, from very low degradation to the complete loss of cement integrity. Furthermore, one study of well cement that underwent 30 years of CO_2 exposure in the SACROC field (CO_2-EOR well) was conducted recently [9,10]. The study shows that Portland cement retained its structural integrity after 30 years in the near-CO_2-reservoir environment, although significant carbonate mineralization above the cap-rock was observed. However, the timescale for all these studies of laboratory-tested cement or field-cement samples ranges from a few hours to a few years. For CO_2 storage, information on cement durability over thousands of years is required. To model long-term cement durability in such severe environments, accelerated degradation methods must be considered and developed.

In the building industry or for radioactive waste repository, some accelerated ageing methods have been developed to model the ageing of concrete over time. One method consists of the application of a voltage through a cement-based material. It has been shown that such a method developed and used by different institutes can be a good technique to accelerate cement degradation [11–13]. The protocol has clearly shown its efficiency and reliability by the quantification of the accelerated chemical and mechanical ageing process due to the application of such potential through cementitious material. The question arises here whether this method could be adapted for CO_2 storage. The main objective of this study is thus to demonstrate if it is possible to accelerate well cement degradation in the presence of CO_2 fluids by using the principle of this accelerated ageing method.

The efficiency and reliability of this approach has clearly been proven since both teams have described and quantified very similar processes indicating accelerated ageing. Furthermore, such method appeared to us as the most appropriate to adapt it by adding CO_2 to the previous protocol.

This paper first presents the setup developed for accelerated degradation tests as well as the materials and the methods used to characterize the degradation of cement. Then, some experimental data obtained on the mechanisms of cement degradation when applying a voltage through a cement sample with and without CO_2 fluids are provided. Finally, the effects of increasing the potential gradient, the temperature of the CO_2-bearing electrolyte, and the CO_2 concentration in the electrolytes on the accelerated cement degradation are presented and discussed.

---

* Corresponding author. Tel.: +33 1 45 37 21 02; fax: +33 1 45 37 25 13.
E-mail address: VBarlet@clamart.oilfield.slb.com (V. Barlet-Gouédard).

0008-8846/$ – see front matter © 2010 Elsevier Ltd. All rights reserved.
doi:10.1016/j.cemconres.2010.03.019

2. Experimental set-up and procedure, materials, and characterization of cement alteration

2.1. Leaching induced by a forced transport in CO_2-rich environment ($LIFTCO_2$) procedure

Some investigations on accelerated ageing methods have shown that the application of a potential gradient through a cement-based material can accelerate its degradation [11–13]. The method consists of the placement of a cement sample between two cells containing water and in which electrodes are immersed, an anode (positive electrode) and a cathode (negative electrode), providing a potential gradient across the specimen (Fig. 1). Both electrodes are connected with a current meter. Following electrochemical theory, when applying a potential gradient to an electrolyte, migration of cations towards the cathode and anions towards the anode occurs. This phenomenon is called the electrophoresis. Thus, the cations from the cement phases (mainly Ca^{2+}) are transported from the cement sample toward the cathode, and the anions (OH^-) are transported toward the anode. The voltage induces a leaching of the cement sample by a forced transport (LIFT; [13]) of the cement ionic species. This voltage-driven transport creates a chemical instability that generates the dissolution and progressive decalcification of the cement phases [11–13].

The setup developed for this study is shown in Fig. 1. The vessel is composed of two cells, each with a volume of about 1500 mL. A removable sample holder is located in the middle of the vessel. Each cylindrical sample is wrapped with rubber tape to ensure a good contact with the sample holder surfaces. This precaution allows good isolation of the two electrolytes and ensures that the ionic species will migrate only across the sample. To decrease the evaporation of the electrolyte, a plate is put on top of the vessel. The experiments are performed under atmospheric pressure. A heating device allows performing the experiments from ambient temperature to 50 °C. The electrodes provide a voltage that can be set between 10 V and 30 V. During a test, the intensity is continuously measured by a current meter and recorded by a nearby computer. The electrolyte is distilled water. In solids, the electrons ensure the flow of electricity. In contrast, in fluids, the ions allow the transport of electricity. The transport of a current from a solid (electrode) towards a liquid phase (electrolyte) is achieved by means of electrochemical reactions at the electrodes. Water electrolysis is a major reaction that occurs at the electrodes (Fig. 1).

The reactions are:

- At the cathode (negative electrode):

$$2.H_2O + 2.e^- \rightarrow H_2 + 2.OH^- \tag{1}$$

- At the anode (positive electrode):

$$H_2O \rightarrow 2.H^+ + 0.5.O_2 + 2.e^- \tag{2}$$

Both reactions at the cathode and at the anode give the equation:

$$H_2O \rightarrow H_2 + 0.5.O_2 \tag{3}$$

Use of stainless steel electrodes avoids any corrosion, particularly water electrolysis-related oxidation of the anode.

The LIFT procedure described previously is combined with a CO_2 supply system for the $LIFTCO_2$ procedure. A CO_2 bottle is connected to the system to provide a flow of CO_2 to the electrolytes of the vessel. A series of electrovalves are controlled by a CO_2 delivery device, which allows setting the amount of CO_2 to be delivered through bubblers immersed in the electrolytes of each cell (Fig. 1).

For most of the tests, the CO_2 bubbling is activated by the CO_2 delivery control device for 30 s every 10 min. The CO_2 flow is set with flow-meters for each chamber, typically either at 25 mL/min or at 100 mL/min.

2.2. Material preparation

Portland cement (Class G, 1.89 SG slurry density) is used for the experiments. The cement samples are prepared using conventional additives as antifoam agent and dispersant. The cement slurry is thoroughly degassed and cement is set at atmospheric pressure and ambient temperature during two weeks. Then the set cement is cored and cut to reach a cement disc of 5 cm diameter and 2.5 cm height. After the experiments, the cement disc is carefully cored to get four cylindrical samples of 1.25 cm diameter and 2.5 cm height (Fig. 2). These samples are used for the distinct analyses. Before and after the experiments, the samples are stored in distilled water.

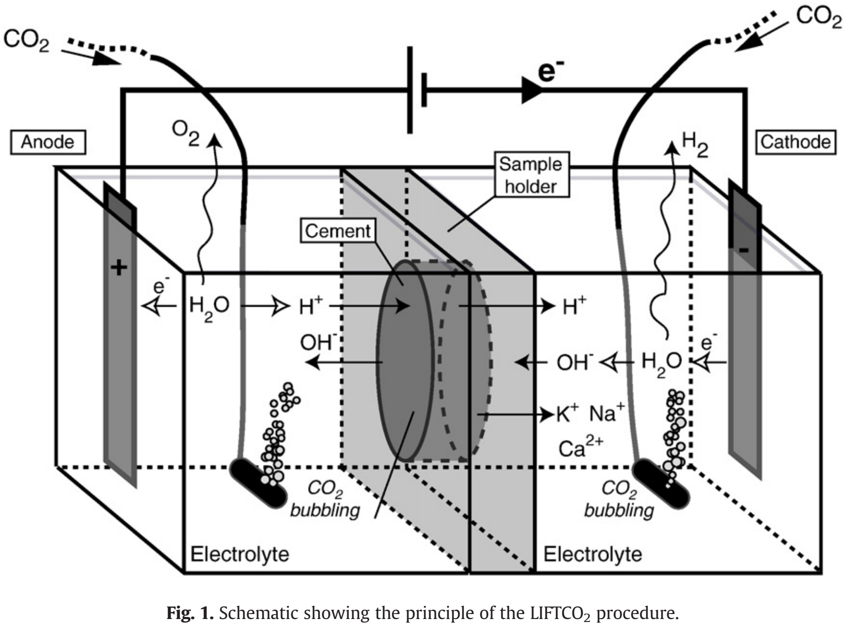

Fig. 1. Schematic showing the principle of the $LIFTCO_2$ procedure.

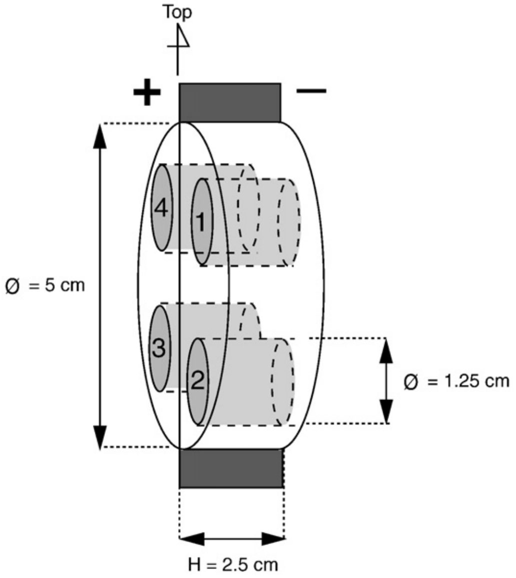

Fig. 2. Schematic showing preparation of the samples from the cement disc attacked with the LIFTCO$_2$ procedure.

2.3. Characterization of the alteration

2.3.1. pH, CO$_2$ concentration evolution and electric current intensity evolution

Before the test, the pH of the fluid (water or brine) in equilibrium with the samples is measured. During the experiment, the pH of the fluid in which the samples are tested is regularly measured. The samples tested in the vessel are then stored in water or brine, and the pH of this solution is measured at equilibrium. Furthermore, the concentration of CO$_2$ dissolved in water is regularly measured with a specific CO$_2$ electrode. For these experiments, three calibrated solutions are prepared at the concentrations 10^{-3}, 5×10^{-3}, and 10^{-2} mol/L of CO$_2$.

A current meter measures the evolution of the electric current intensity in the electrolyte every minute. The electric conductivity of a solution is directly linked to its ionic composition. During a test, the electric conductivity of water increases, which is related to the amount of leached cement ionic species that progressively increases with time. The evolution of the current at the cement edges is thus controlled by the electrolyte conductivity.

2.3.2. Aspect of the samples

All the samples are measured (weight, dimensions) and photographed before and just after the test in the LIFTCO$_2$ vessel.

The density of the core samples is measured by dividing its weight by the weight of the displaced volume of water.

Furthermore, polished sample cross sections are made to measure the thickness of the alteration front.

2.3.3. Mineralogical evolution and microstructural characterization

For mineral-phase identification in the different zones of the samples, pieces (10 to 50 mg) are extracted from the edges and the centre of the samples (anode side, cathode side and central part). Then the sample pieces are ground for powder X-ray diffraction (XRD) analyses with a D5000 SIEMENS diffractometer.

Furthermore, samples are cut to make polished thin sections in the longitudinal diameter plane of the core sample. Scanning Electron Microscope (SEM) observations are performed on these sections in secondary electron (SE) or back-scattered electron (BSE) modes to obtain information on the alteration process. A Hitachi S-3400/N instrument coupled with an EDS device (NORAN system SIX model from ThermoElectron corp.) is used. For the EDS analyses, the following elements are consistently measured: Mg, Al, Si, S, Ca, and Fe.

2.3.4. Porosity evolution

Mercury Intrusion Porosimetry (MIP) is used to evaluate the porous space over a broad range (theoretically from 0.003 µm to 360 µm). The common procedure consists of drying the specimen to empty the pores of any existing fluid, then weighing the sample and transferring it to the measurement cell. After the air in the cell is evacuated, the cell is filled with mercury. Since mercury is a non wetting fluid, it does not enter into the specimens, unless pressure is applied. Pressure in progressive increments is applied to the mercury, and the corresponding intruded volumes are monitored. Two intrusion–extrusion cycles are performed to determine irreversible and reversible intrusion volumes. The maximum intrusion pressure is about 4100 bars. Therefore, the results obtained represent the porosity filled with mercury at this pressure, i.e., the volume of cavities connected to the surface through a path with a diameter greater than 3 nm. Detailed description of the method as well as its application on cementitious material is reported in Rimmelé et al. (2008) [3].

3. Results with the LIFT procedure

Two tests were performed on Portland cement set under atmospheric pressure and ambient temperature using the LIFT procedure (without CO$_2$), during 4 days (Test 1) and 5 weeks (Test 2), with a voltage set at 10 V (Table 1). For both samples tested during 4 days and 5 weeks, the variations of the weight, density, and dimensions are lower than 1%, which is in the range of the measurement accuracy. Samples cut along their diameter exhibit an alteration front at the cathode side, after both 4 days and 5 weeks of testing (Fig. 3). At the anode side, a front is also visible but it appears thinner than that at the cathode side.

At the microscopic scale, one can notice that the kinetics of degradation is given by the kinetics of the advancing alteration front with time. The mechanisms involved with this LIFT procedure are mainly linked to the forced transport of the ionic species, the diffusion process being too slow to be considered. This forced transport creates, at the cathode side, the dissolution of portlandite and progressive decalcification of the cement phases. This is particularly visible after 5 weeks of experiments. EDS analyses show that the alteration front at both anode and cathode sides does not contain portlandite, and the initial C–S–H phases have lost their calcium content (Fig. 4). The difference between both sides is that at the cathode side, the calcium has been leached from the cement sample and released in the electrolyte. Furthermore, cracking is visible and localized in the front (at the anode

Table 1
Conditions of tests performed on Portland cement set under atmospheric pressure and at 20 °C and tested with the LIFT or LIFTCO$_2$ procedure. The CO$_2$ bubbling, when applied into the cell, lasts 30 s.

Test name	Test temperature (°C)	Voltage (V)	CO$_2$ flow in each cell (ml/min)	CO$_2$ bubbling frequency (min)	Test duration (week)
1	20	10	0	10	0.5
2	20	10	0	10	5
3	20	0	25	10	1
4	20	0	25	10	3
5	20	10	25	10	1
6	20	10	25	10	3
7	20	30	25	10	1
8	20	30	25	10	3
9	40	10	25	10	3
10	20	30	25	10	1
11	20	30	100	1	1
12	20	30	25	10	3
13	20	30	100	10	3
14	20	30	100	1	3

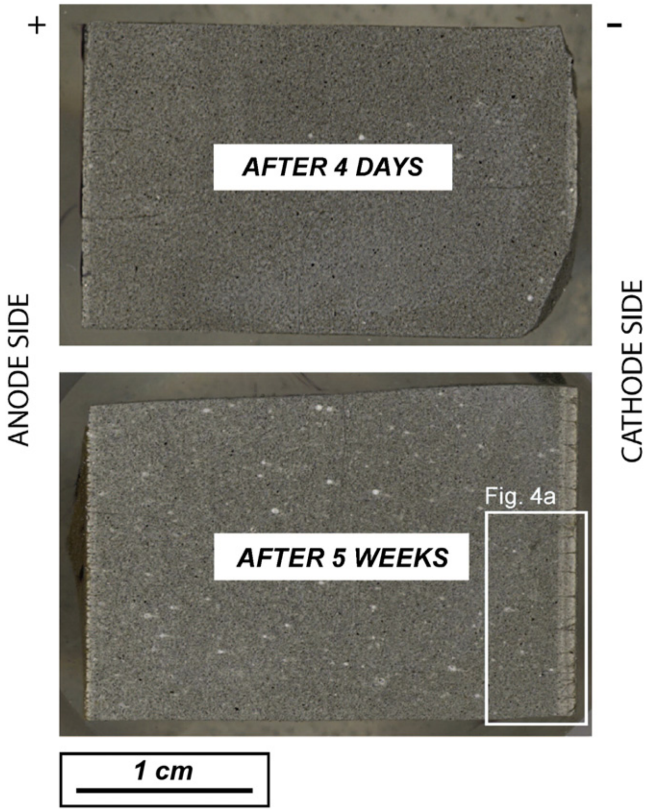

Fig. 3. Cross sections of the samples tested with the LIFT procedure, with a potential gradient of 10 V, during 4 days and 5 weeks.

and cathode sides), perpendicular to the cement surface. Some dissolution patterns around these cracks (Fig. 4) attest that these cracks are related to the forced transport and do not come from sample preparation. Similar radial cracks have been observed by Gérard [13]. Deeper in the sample, beyond the altered zone, portlandite occurs widely, as detected by XRD and SEM analyses.

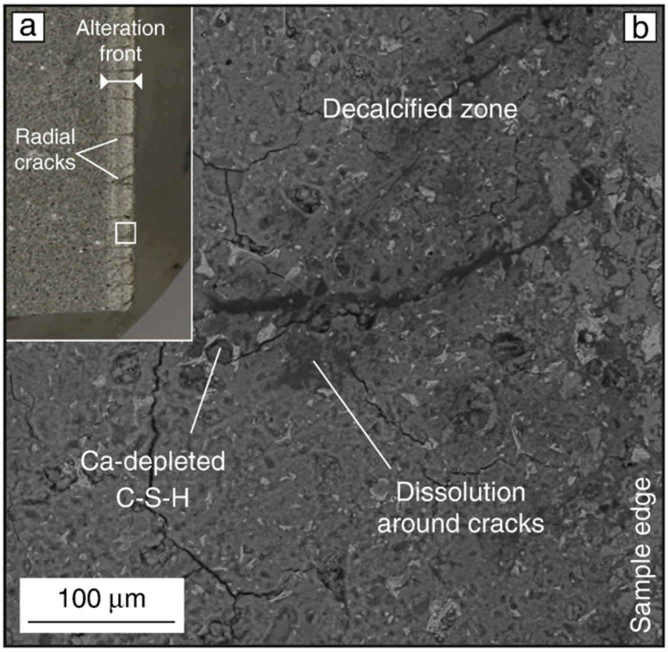

Fig. 4. Cross section (a) showing the location of the SEM-BSE image (b) at the cathode side of the sample tested with the LIFT procedure during five weeks.

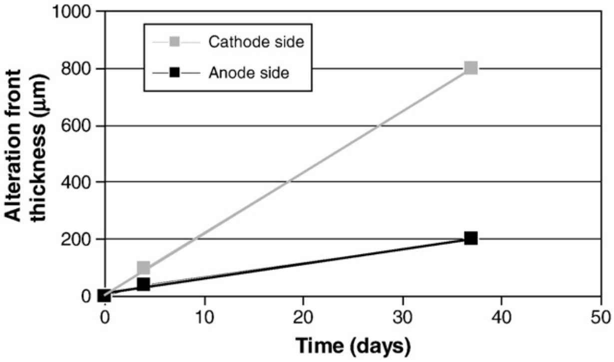

Fig. 5. Evolution of the alteration front thickness measured at the anode side and at the cathode side on samples tested with the LIFT procedure during 4 days and 5 weeks.

The scanning electron microscopy on these samples allows quantifying precisely the thickness of these fronts (Fig. 5). After 4 days, the uniform alteration front is about 40-µm thick at the side located in front of the anode, whereas it is 100-µm thick at the cathode side. After 5 weeks, the altered zone is about 200-µm thick at the anode side, whereas it reaches 800 µm at the cathode side. The altered zone thickness is thicker at the cathode side than at the anode side, and the kinetics of cement degradation when applying a voltage is proportional to the time of exposure. Saito et al. [11], with a roughly similar set up, found that the application of a potential gradient of 25 V to a mortar specimen accelerated dissolution of the calcium ionic species from cement hydrates to a rate of about 60 times higher than that of a system in which water is renewed from time to time under no potential gradient. Furthermore, Gérard [13] also reported similar observations, and estimated an accelerating rate of 100 (with a potential gradient of 10 V), this rate being calculated in terms of duration required to reach a similar thickness of alteration front, with or without voltage.

To summarize, the two Portland cement samples exposed to a potential gradient of 10 V during 4 days and 5 weeks at atmospheric pressure and room temperature show a leaching due to the forced transport of the cement ionic species. The leaching is restricted to a uniform alteration front in which portlandite is dissolved and the C–S–H phases are decalcified. This decalcified zone is 4 times thicker at the cathode side than at the anode side, which is related to the potential-driven transport of the cement cations towards the negative electrode (cathode). Radial cracking is associated with the leaching of the cement ionic species. The depth of attack increases linearly with time and is thus not a diffusion-controlled process.

The following section describes the impact of providing a CO_2 bubbling on the acceleration of cement degradation related to the application of a potential gradient using the LIFTCO_2 procedure.

4. Results with the LIFTCO_2 procedure

To study the effect of applying a voltage across a cement sample in CO_2-rich fluids (LIFTCO_2 procedure), six tests (Tests 3 to 8; Table 1) have been performed with the LIFTCO_2 vessel. For all the six tests, Portland cement is exposed to CO_2 environment at atmospheric pressure and temperature of 20 °C. The CO_2 flow in each cell is set with the flowmeter at 25 mL/min in each chamber, and the frequency of bubbling is activated for 30 s every 10 min. The test durations are 1 week and 3 weeks, and the voltage is set at 0, 10, and 30 V to investigate the effect of increasing the voltage on the acceleration of the degradation (Table 1).

4.1. pH, CO_2 concentration and electric current intensity evolutions

Before the experiments, the pH of the electrolyte at the equilibrium with the sample equals about 12. During all the experiments, the pH of the electrolyte drastically decreases from 12 to 5 in the first hours of test.

For the test without voltage, it remains equal to 5 to 6 in both cells. For the experiments performed with a 10 V potential gradient, the pH at the anode remains stable at 5 whereas that at the cathode is stable at a higher value (pH ~ 6). At higher voltage (30 V), this pH gradient between both electrolytes is more significant (pH equals 4 in the anode cell versus 6 in the cathode cell). This higher pH in the cell with the cathode may be explained by the production of OH^- at the cathode (inducing higher pH) and H^+ at the anode (inducing lower pH) by water electrolysis. As the voltage is higher, more OH^- ions are produced at the cathode, increasing the pH, and more H^+ ions are produced at the anode, decreasing the pH (to 4).

When a potential gradient is applied, after few days of experiments, the CO_2 concentration reaches a plateau at 2×10^{-2} mol/L in the cathode electrolyte and 1×10^{-2} mol/L in the anode electrolyte (Fig. 6). The lower CO_2 concentration in the anode electrolyte than in the cathode electrolyte was observed with all the experiments when a potential gradient was applied. It may be related to the fact that most of the reactions involving dissolved CO_2 with Ca^{2+} from the cement occur in the cathode cell, and there is thus a higher availability of carbonic species in that electrolyte. Another explanation, which is the most likely, involves the solubility of CO_2 that increases with the pH. As mentioned earlier the pH is higher in the cathode cell, and thus more CO_2 may be dissolved in the cathode electrolyte.

For a 10 V test, the current density increases to 1.0 mA/cm^2 in the first day and reaches 1.5 mA/cm^2 after 3 days. For a 30 V test, it rapidly increases to 5.0 mA/cm^2 in the first day and reaches 5.5 mA/cm^2 after a few days. Since the electric conductivity is directly linked to the ionic composition of the electrolytes in both cases, this evolution shows that the amount of leached cement ionic species is significant during the first day of the experiment.

4.2. Aspect of the samples

For the six tests, the variations of the weight, density, and dimensions are lower than ± 1%, which is in the range of the measurement accuracy.

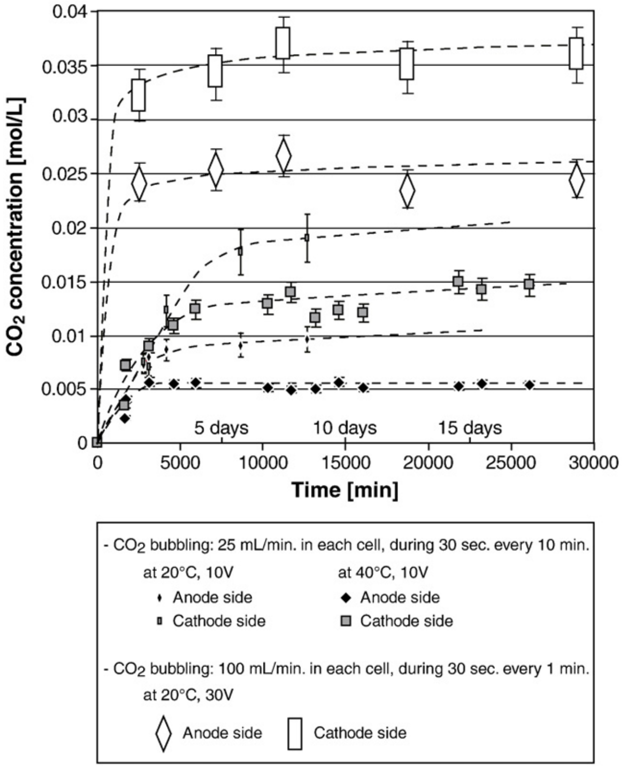

Fig. 6. Evolution of the CO_2 concentration with time of both electrolytes, for tests performed at different temperature and at different amount of CO_2 bubbling, during 3 weeks.

At both the anode and cathode sides of the exposed samples, with and without applying a potential gradient, the cement surfaces exhibit a brownish color. Cement has thus reacted on both sides with the ionic species occurring in the electrolyte. Furthermore, for the test performed at high voltage during 3 weeks (Test 8), the cathode is covered by a whitish mineral layer, while the anode remains free of precipitate (Fig. 7A). X-ray diffraction analysis of the crystals precipitated at the surface of the cathode reveals the occurrence of calcite and vaterite (Fig. 7B). Both calcium carbonate polymorphs come from the reaction of the Ca^{2+} ions leached from the cement and transported towards the cathode, with the carbonate ionic species coming from the dissolution of CO_2 in the electrolyte.

4.3. Mineralogical evolution and microstructural characterization

4.3.1. X-ray diffraction spectroscopy analyses

XRD analyses were performed on the whole set of Portland cement samples exposed to CO_2 bubbling alone, to CO_2 and a 10 V potential gradient, and to CO_2 and a 30 V potential gradient, during 1 week and 3 weeks (Table 2). Sound Portland cement is mainly made of portlandite, C2S, C3S, brownmillerite, a very low amount of calcite (relict of the clinker), and C–S–H phases. After the 1-week and 3-week experiments with CO_2 alone, calcite has formed at the edges of the samples by the reaction of portlandite and the C–S–H phases with CO_2. The middle part has the composition of a sound sample. For the tests with an applied voltage, a clear dissolution of Portlandite and the calcium silicate phases is detected at the cathode side. Furthermore, calcium carbonate polymorphs (calcite and vaterite) have precipitated. This is especially well detected for the longest durations of exposure and the highest voltage, for which the ionic transport is significant. In contrast, no major reaction occurs at the anode side, as most of portlandite is preserved at the surface of the samples and a low amount of calcite precipitates.

4.3.2. Microstructural analyses and front thickness estimates

The cross sections of the six samples (Fig. 8) allow the detection of a front at the edges of each sample, at the anode side and at the cathode side. Except for the tests without application of a potential gradient, the front thickness appears systematically greater at the cathode side of the samples than at the anode side.

At fixed conditions (0, 10 or 30 V), the cross sections show that the thickness of the alteration front increases with the duration of exposure (Fig. 8). Furthermore, at a fixed duration, the thickness of this alteration front also increases with the voltage.

Therefore, at this stage, it can be emphasized that in a CO_2-rich environment, the application of a potential gradient through a cement sample accelerates the penetration of this front. The higher the voltage, the deeper the front penetrates into the sample.

The polished sections of the samples were examined under scanning electron microscope to investigate the process of alteration and to measure thoroughly the thickness of the distinct alteration fronts.

For the samples exposed to CO_2 bubbling alone (0 V), at both edges of the samples, SEM-BSE observations show that the alteration front is composed of a series of fronts with different porosity and mineralogy. From the edge towards the inner part of the sample, one can observe a gel layer, a carbonation front, and a dissolution front (Fig. 9a). A similar alteration pattern has already been described for Portland cement samples tested in autoclaves under simulated pressure and temperature downhole conditions [1–3]. The gel layer contains few calcium carbonate, silica gel, and calcium-depleted calcium silicate phases. Ahead of this zone, the carbonation front is a thin front of very low porosity (as seen on SEM-BSE images), in which abundant calcium carbonates have precipitated. The carbonation front contrasts with the dissolution front, which is a zone of high porosity where Portland cement phases (portlandite and calcium silicate hydrate phases) progressively dissolve to form calcium carbonates backwards, in the carbonation front. Indeed, dissolution of the cement hydration products

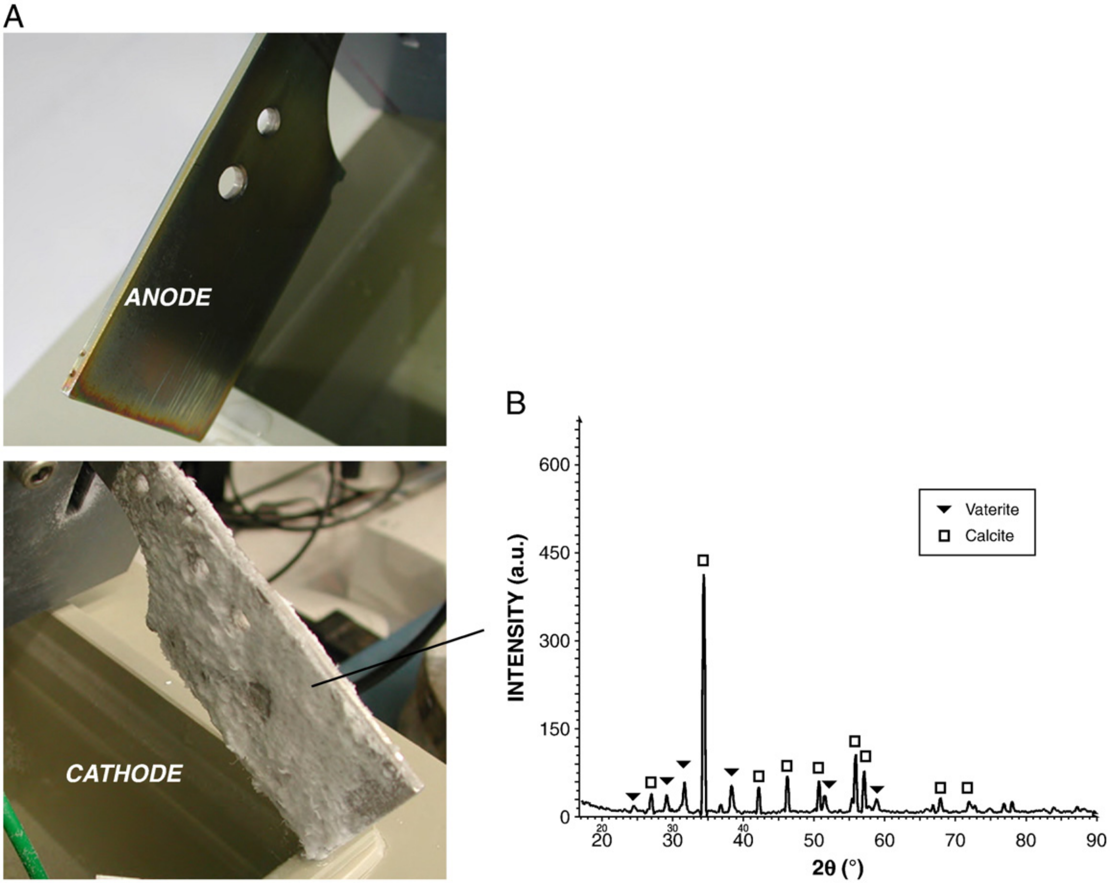

Fig. 7. (A) Pictures showing the state of the positive (above) and negative (below) electrodes after a CO_2 test performed during 3 weeks at 30 V (Test 8). (B) X-ray diffraction analysis of the crystals precipitated at the surface of the cathode.

provides OH^- and Ca^{2+} ions toward the carbonated area. After 1 week, the total thickness of this series of front (the so-called “Alteration Front”) is about 300 to 350 µm (Table 3). After 3 weeks, it is of about 600 µm. For comparison, the thickness of this alteration front in Portland cement tested with the LIFTCO$_2$ procedure under atmospheric pressure and at 20 °C is about 10 times lower than that in Portland cement tested in batch experiments at 280 bars and 90 °C [1–3]. Both the material properties and the pressure and temperature conditions, which differ between both types of experiments, may explain this factor of 10. On one hand, for the LIFTCO$_2$ procedure, Portland cement has set under atmospheric pressure and ambient temperature, resulting in a lower permeability and porosity than for a Portland cement cured under pressure and at higher temperature. This may be responsible for a lower attack at room temperature than at higher temperature. For instance, the porosity of the cement set under atmospheric pressure and room temperature is about 28%. That for a similar Portland cement cured at 90 °C and 3000 psi is about 35% [3]. On the other hand, under atmospheric pressure and ambient temperature, the solubility of CO_2 is drastically lower than at 280 bars and 90 °C, with pressure being mainly responsible for such difference of solubility [14–17].

For the samples exposed to CO_2 bubbling and a potential gradient of 10 V, a similar pattern of alteration is observed at the cathode side (Fig. 9b). Calcium-depleted C2S and C3S, as well as silica gel, are observed in the gel layer. The alteration front is about 600 µm after

Table 2
Main mineral phase occurrences obtained by X-ray diffraction spectroscopy for the tests performed with CO_2 alone, with CO_2 and a 10 V potential gradient, and with CO_2 and a 30 V potential gradient, during 1 week and 3 weeks.

Test name	0	3		5			7			4		6			8		
Conditions	Initial	1 week in CO_2-saturated water								3 weeks in CO_2-saturated water							
		0 V		10 V			30 V			0 V		10 V			30 V		
Location of XRD analyses in the sample	Middle	Edges	Middle	Anode side	Middle	Cathode side	Anode side	Middle	Cathode side	Edges	Middle	Anode side	Middle	Cathode side	Anode side	Middle	Cathode side
Portlandite	+	x	+	+	+	x	+	+		x	+	+	+		+	+	
C_2S	+	x	+	+	+	+	+	+		x	+	x	+	x	x	+	
C_3S	+	x	+	+	+			+		x	+	+	+			+	
Calcite		x				x	x		+	x		x		+	x		+
Vaterite									+					+			+

+ abundant mineral phase; x mineral phase in low amount.

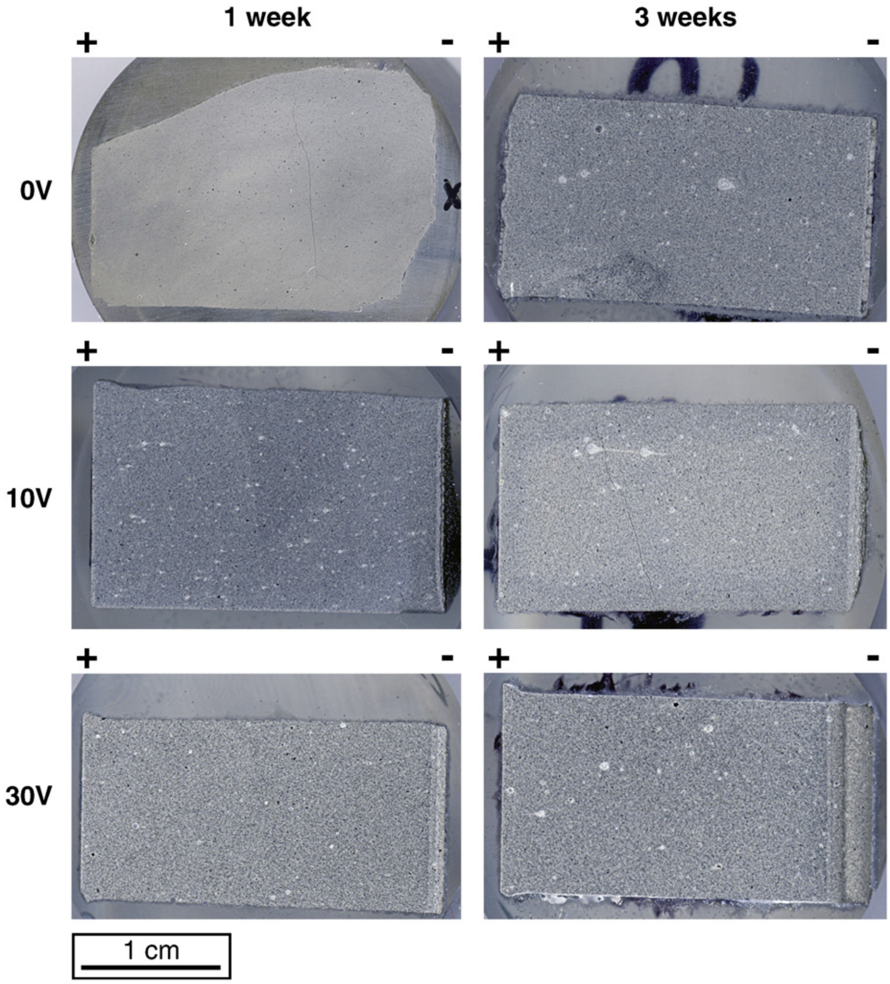

Fig. 8. Cross sections of the samples tested at 0 V, 10 V, and 30 V during 1 week and 3 weeks. The cathode side and the anode side of the samples are located with the − and + symbols, respectively.

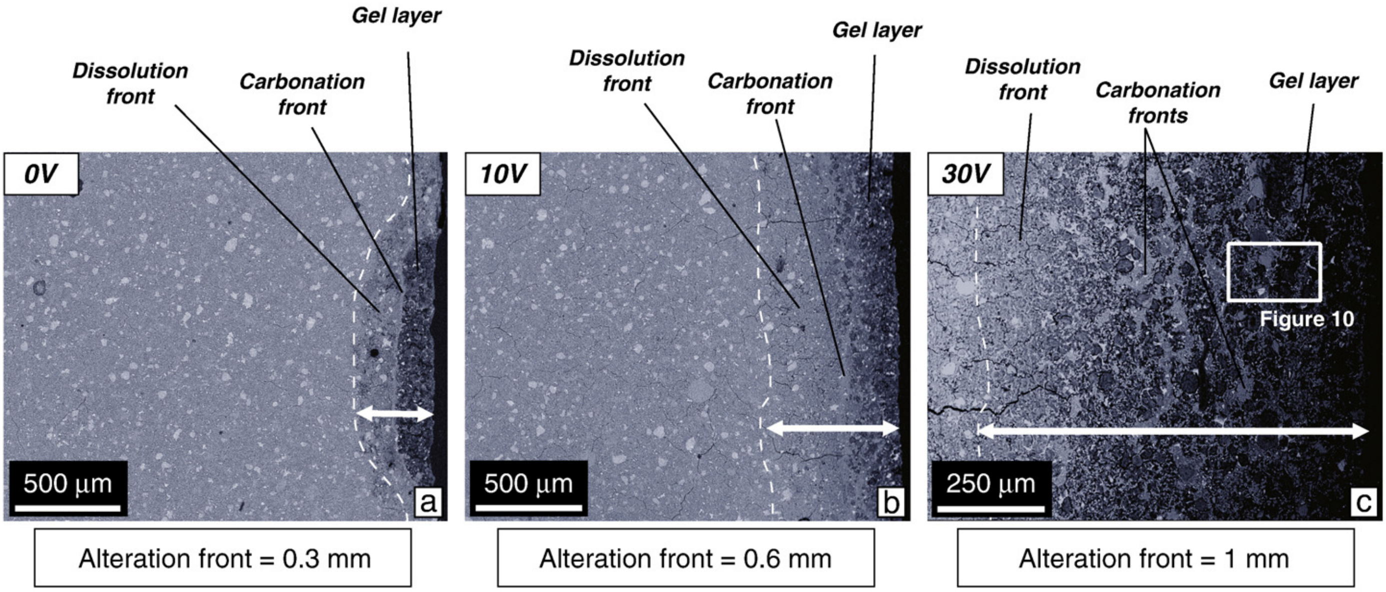

Fig. 9. SEM-BSE images showing the alteration front pattern and thickness estimates at the cathode side for a Portland cement tested at 0 V (a), 10 V (b) and 30 V (c) during 1 week in CO_2-saturated water. Location of Fig. 10 is reported.

Table 3
Thickness of the different fronts in the altered zone at the cathode side; the thickness of each front is measured on several SEM-BSE images. The thickness of the entire altered zone is reported in the last column (alteration front = gel layer + carbonation front + dissolution front).

Test name	Conditions	Gel layer (μm)	Carbonation front (μm)	Dissolution front (μm)	Alteration front (μm)
3	0 V, 1 week	150–170	10	150–170	350
5	10 V, 1 week	250	50	300	600
7	30 V, 1 week	600–700		300	950
4	0 V, 3 weeks	250–350	10–20	250	600
6	10 V, 3 weeks	500–550	200	450–500	1200
8	30 V, 3 weeks	2000–2100		700–800	2800

Table 4
Thickness of the different fronts in the altered zone at the anode side; the thickness of each front is measured on several SEM-BSE images. The thickness of the entire altered zone is reported in the last column (alteration front = gel layer + carbonation front + dissolution front).

Test name	Conditions	Gel layer (μm)	Carbonation front (μm)	Dissolution front (μm)	Alteration front (μm)
3	0 V, 1 week	150–170	10	150–170	350
5	10 V, 1 week	0	0	0	0
7	30 V, 1 week	100	0	0	100
4	0 V, 3 weeks	250–350	10–20	250	600
6	10 V, 3 weeks	0	0	0	0
8	30 V, 3 weeks	100	0	0	100

1 week and 1200 μm after 3 weeks of exposure (Table 3). Furthermore, cracking is commonly localized in the carbonation front and dissolution front. It is related to the combination of cement carbonation and leaching of the cement ionic species with the voltage application. At the anode side, thin sporadic layers of calcium carbonate (about 100 μm) have precipitated (Table 4). Neither carbonation front, nor dissolution front or gel layer can be seen.

For the samples exposed to CO_2 bubbling and a potential gradient of 30 V, the alteration front thickness at the cathode side increases from about 1000 μm after 1 week to 2800 after 3 weeks (Fig. 9c; Table 3). Nevertheless, the alteration front is made of a dissolution front and a zone with intercalated carbonation fronts and dissolution zones. In this more diffuse zone, a carbonation gradient occurs with increased carbonation toward the edge of the sample, and a dissolution gradient occurs with increased dissolution toward the inner part of the sample. Close to the edge of the sample, calcium-depleted C2S and C3S, silica gel, and calcium carbonate occur (Fig. 10). At the anode side, a dissolution zone of about 100-μm thickness is observed at both durations (Table 4). Intense cracking occurs at both edges of the samples tested with 30 V of potential gradient, and is attributed to the leaching of the cement ionic species when applying such voltage.

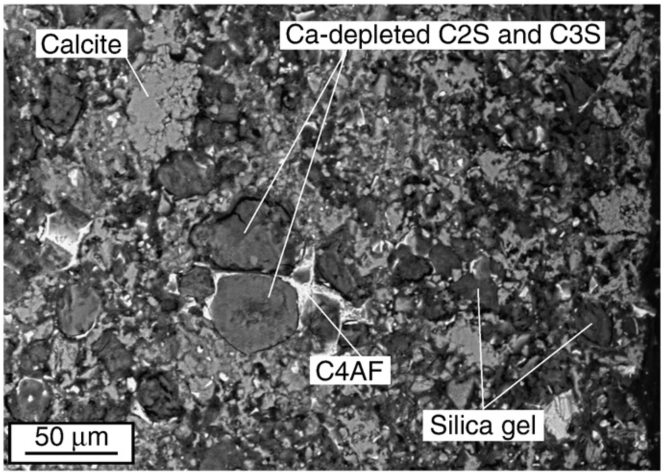

Fig. 10. SEM-BSE image showing the reaction products of cement with CO_2, in the gel layer, after 1 week of exposure at 30 V in CO_2-saturated water. Location of this picture is shown at a wider scale in Fig. 9.

4.3.3. Acceleration rates

Fig. 11 plots the evolution of the alteration front thickness with time, the evolution of the dissolution front thickness with time, and the evolution of the thickness of the combined carbonation front and the gel layer with time, all being measured at the cathode side by SEM analyses (Table 3).

Fig. 11a shows that the application of a potential gradient across a sample in CO_2-saturated water accelerates its alteration. Increasing the voltage clearly accelerates the cement alteration. Furthermore, the diffusion process seen in the test with CO_2 alone becomes progressively negligible with the tests at 10 V and 30 V. The forced transport process induced by the voltage application becomes the major process, especially when a high potential gradient is applied.

Fig. 11b and c show that at 30 V, the evolution of the penetration depth for the dissolution front with time and that of the carbonation front and gel layer are proportional to the duration of exposure. They are totally controlled by the forced transport of the ionic species and are not governed by any diffusion process, as is the case for a test without the application of a voltage (evolution proportional with $\sqrt{t}$).

The curve of Fig. 11a allows assessing first-order alteration accelerating rates. They are estimated in terms of duration required to have a similar thickness of alteration front, with or without voltage. The accelerating rate is about 3 between a test without voltage and one with a 10 V potential gradient (similar front thickness after 3 weeks without voltage and after 1 week under 10 V). The accelerating rate is about 6 between a test without voltage and one with a 30 V potential gradient (similar front thickness after 3 weeks without voltage and after half a week under 30 V). Nevertheless, if one considers much longer tests at 0 V compared to the short one at 30 V, the diffusion-controlled process may imply much greater accelerating rate.

Finally, in the case of no CO_2 bubbling applied to the system (LIFT procedure under a voltage of 10 V in pure water), an alteration front 400-μm thick at the cathode side can be deduced from the curve of Fig. 5. After 3 weeks with the LIFTCO_2 procedure with a 10 V potential gradient, the thickness of the alteration front (although of a different nature) is about 1200 μm, i.e., 3 times greater. The LIFTCO_2 procedure therefore involves more severe process than the LIFT procedure for the degradation of Portland cement.

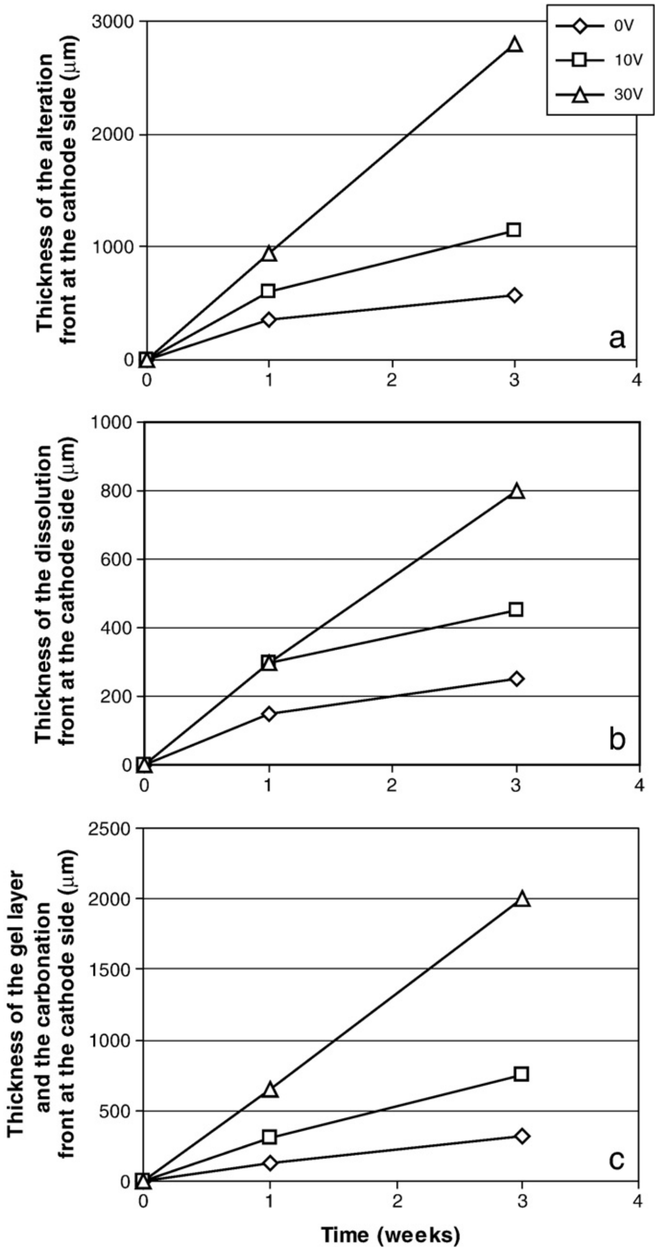

Fig. 11. Evolution of the whole alteration front thickness (a), the dissolution front (b) and the gel layer and carbonation front (c) with time, observed at the cathode side of the samples tested in CO_2-saturated water, with a voltage of 0 V, 10 V, and 30 V, during 1 week and 3 weeks.

4.4. Porosity evolution

The evolution of the porosity with time, deduced from mercury intrusion porosimetry measurements, is shown in Fig. 12. For the samples tested without voltage, the porosity decreases from 27% to 20% after 1 week, and increases between 1 week and 3 weeks up to the porosity value of 30%. A very similar evolution with porosity values of the same order of magnitude is observed for the samples tested at 10 V. In contrast, the samples tested at 30 V show an evolution with an increasing porosity from 27% to 31% after 1 week and to 32% after 3 weeks. A test at longer duration may be useful to see if the porosity continues to increase with time at high voltage or if it stabilizes as it seems to do after 3 weeks.

Therefore, the evolution of the porosity shows that the higher the voltage, the higher the dissolution; forced transport of the cement species occurs and, therefore, the porosity increases with time.

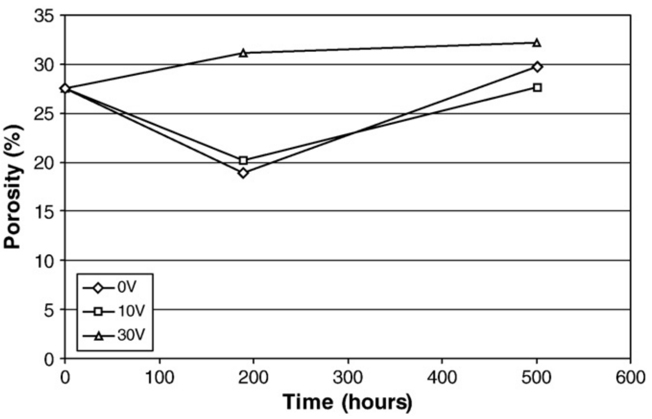

Fig. 12. Evolution of the porosity deduced from mercury intrusion porosimetry analyses, for the samples tested with the LIFTCO$_2$ procedure during 1 week and 3 weeks, at 0 V, 10 V, and 30 V.

5. Accelerating effect of increasing the temperature in the LIFTCO$_2$ procedure

To study the effect of temperature on the acceleration of the cement degradation under CO_2 environment, a heating device was installed to launch a test with a voltage of 10 V at 40 °C. The cement sample set under atmospheric pressure and ambient temperature. The CO_2 flow in each cell is set at 25 mL per minute in each chamber, and bubbling is activated for 30 s every 10 min (Table 1). The test duration is 3 weeks (Test 9) and will be compared with a test performed at lower temperature (Test 6).

5.1. pH, CO_2 concentration and electric current intensity evolutions

During the experiment, the pH of the electrolytes at 40 °C shows a similar evolution to that at 20 °C. At the beginning of the test, the pH of the electrolyte decreases from 12 to about 5. Then, during the tests, the pH at the anode remains stable at the value of 5 whereas that at the cathode is stable at a higher value (pH ~ 6), which has been interpreted to be due to the effect of water electrolysis at the anode and cathode.

As for a test at 20 °C, the CO_2 concentration is slightly lower in the electrolyte with the anode than in the electrolyte with the cathode (Fig. 6). In the cell with the anode, the concentration increases to 5.10^{-3} mol/L after few days of experiment. In the cell with the cathode, the CO_2 concentration increases to $1.5.10^{-2}$ mol/L in the first days of exposure. Then the concentration reaches a plateau at these values in both cells. Furthermore, whatever the cell, the CO_2 concentration is lower at 40 °C than at 20 °C. This lower concentration – at fixed pressure of exposure – is explained by the lower solubility of CO_2 when increasing the temperature [15].

Although the first-order evolution of the current is roughly of the same trend for the test performed at 40 °C and that at 20 °C, the current reaches 3 mA for the test performed at 40 °C whereas it is 2 mA for the test at 20 °C (Fig. 13). The electrolyte conductivity is therefore higher at 40 °C than at 20 °C, which is explained by the diffusivity of the ionic species that increases with temperature.

Therefore, for this test at 40 °C, compared to that at 20 °C, there are two processes that may have opposite effects on the acceleration of the cement alteration in CO_2-saturated water: there is lower CO_2 available in the electrolyte to react with cement than at 20 °C, but the forced transport of the ionic species is enhanced at 40 °C compared to 20 °C.

5.2. Aspect of the samples

The sample disc surfaces exposed to CO_2-saturated water for three weeks at 40 °C are very similar to those at 20 °C under the same conditions

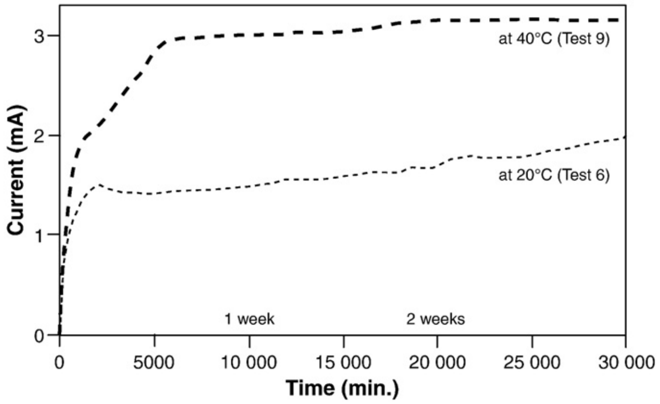

Fig. 13. Effect of temperature (40 °C, above versus 20 °C, below) on the evolution of the current with time for tests performed with the $LIFTCO_2$ procedure, at 10 V during 3 weeks.

of voltage application (10 V). A similar brownish color attesting that cement reacted with both electrolytes is observed.

5.3. Mineralogical evolution and microstructural characterization

5.3.1. X-ray diffraction spectroscopy analyses

X-ray diffraction analyses show that the surface of the cement sample with the strongest reaction is the surface in front of the cathode (Fig. 14). Indeed, at the anode side, a low amount of calcite has formed at the surface of the sample. Relicts of portlandite still occur, which attest that this area has partially reacted with CO_2. However, at the cathode side of the sample, portlandite is not detected, and the analysis reveals formation of both vaterite and calcite. The cement surface in front of the cathode has completely reacted. Deeper in the sample, the cement has the mineralogy of a sound cement.

5.3.2. Microstructural analyses and front thickness estimates

The cross section along the diameter of the sample tested at 40 °C shows an alteration front of about 1.5 mm at the cathode side, thicker than that for the test at 20 °C (Fig. 15). No front appears when focusing at the anode side, similar to the sample tested at 20 °C.

At the microscopic scale, the absence of any front at the anode side is confirmed. Preserved portlandite and calcium silicate anhydrous phases occur. The low amount of calcite detected by X-ray diffraction analysis (Fig. 14) comes from a thin layer of pure $CaCO_3$ having precipitated at the surface, and that layer detached from the sample during sample cross-section preparation for SEM analysis. In the middle of the sample, similar to the anode side, the sample appears well preserved. Portlandite, C2S, and C3S widely occur. Portlandite is particularly well visible in concentric holes that correspond to air bubbles trapped in the slurry. At the side in front of the cathode, a clear alteration front is made of a dissolution front, a carbonated zone and a gel layer. Decalcified C2S and C3S, as well as portlandite dissolution, occur in the dissolution front. The carbonated zone is made of a series of carbonation fronts intercalated with silica gel fronts, all being parallel to the edge of the sample. The dissolution zone is of high porosity and is mainly made of silica gel.

Table 5
Comparison of the thickness of the different fronts in the altered zone at the cathode side, for tests performed at 20 °C and 40 °C. The thickness of the different fronts is measured from several SEM-BSE images. The thickness of the entire altered zone is reported in the last column (alteration front = gel layer + carbonation front + dissolution front).

Test name	Conditions	Gel layer (μm)	Carbonation front (μm)	Dissolution front (μm)	Alteration front (μm)
6	10 V 20 °C 3 weeks	500–550	200	450–500	1200
9	10 V 40 °C 3 weeks	300–350	800	300	1400

The total thickness of this alteration front is 1.4 to 1.5 mm, which is slightly thicker than that for the test at 20 °C (1.2 mm) (Table 5). It is noteworthy that at 40 °C the carbonated zone is thicker than at 20 °C. Such a pattern of alteration, with a more diffuse carbonated zone at 40 °C rather than a thin carbonation front at 20 °C, is similar to the alteration pattern described in the previous section for the tests at higher voltage (30 V; 20 °C).

6. Accelerating effect of increasing the CO_2 bubbling in the $LIFTCO_2$ procedure

The effect of the CO_2 flow and bubbling delivery on the acceleration of cement alteration was studied with the $LIFTCO_2$ vessel. The voltage is set at 30 V for all the tests, the test durations are 1 week and 3 weeks, and the tests are performed under atmospheric pressure and ambient temperature. Different tests were performed with varying CO_2 flow from 25 mL/min. to 100 mL/min., and the CO_2 bubbling frequency from 30 s of bubbling every 10 min to every 1 min, the latter condition corresponding to a quasi-continuous CO_2 delivery into the vessel (Table 1).

6.1. pH, CO_2 concentration and electric current intensity evolutions

For the highest CO_2 delivery into the cells (100 mL/min for 30 s every minute), the pH evolution of the electrolytes is similar to that at

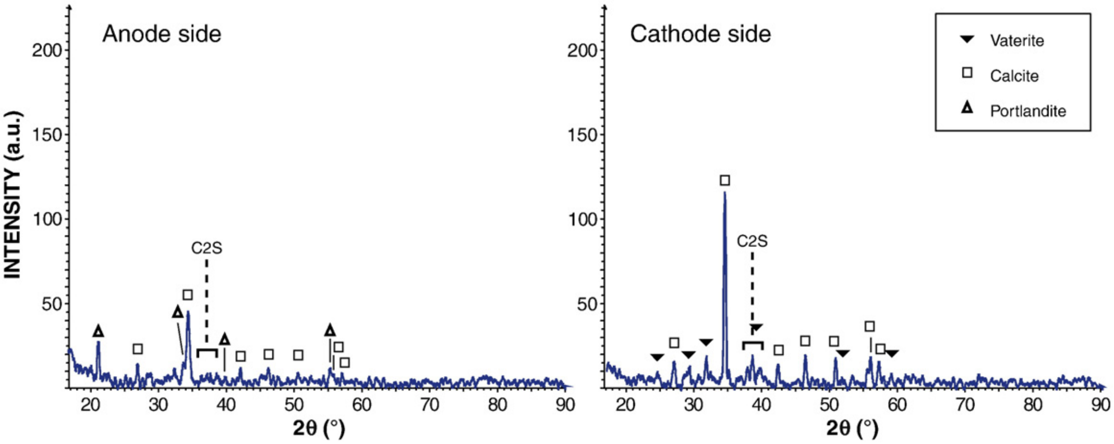

Fig. 14. X-ray diffraction analysis made at both sides of the cement sample exposed to CO_2 at 40 °C, at 10 V, during 3 weeks.

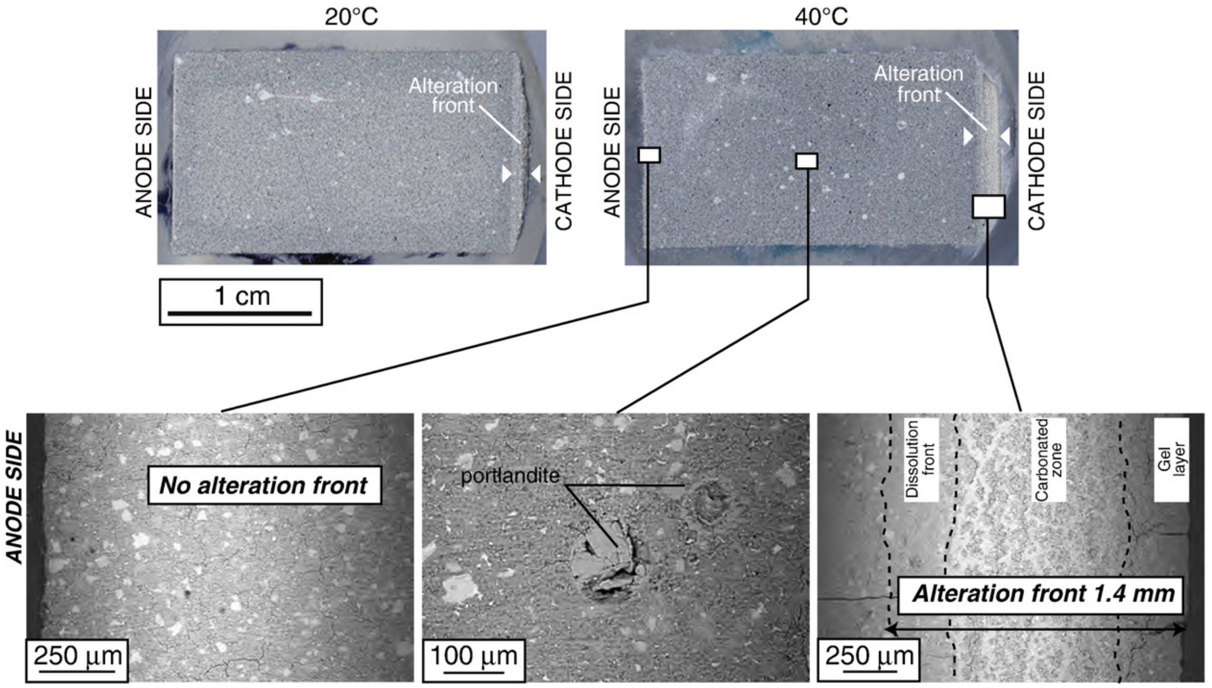

Fig. 15. Above: cross sections of Portland cement samples tested with the LIFTCO$_2$ procedure, at 10 V during 3 weeks, either at 20 °C (left) or at 40 °C (right). Below: SEM-BSE images across the Portland cement sample tested at 40 °C (anode side, middle and cathode side; from left to right).

lower CO$_2$ delivery (25 mL/min. every 10 min.), previously shown for voltage set a 30 V (initial decrease from 12 to 6 and then stable around 6 over time).

The typical evolution of the CO$_2$ concentration measured over time for high CO$_2$ delivery conditions (e.g., Test 14; Table 1) is shown in Fig. 6. The trend is similar to that for tests with lower CO$_2$ bubbling, but the concentrations measured are higher than for conventional CO$_2$ flows (25 mL/min. every 10 min.). In the cathode cell, concentration is 3.5×10^{-2} mol/L (versus 2×10^{-2} mol/L for conventional CO$_2$ bubbling) and 2.5×10^{-2} mol/L in the anode cell (versus 1×10^{-2} mol/L for conventional CO$_2$ bubbling).

The evolution of the current over time is roughly similar regardless of the variation of the CO$_2$ flow and bubbling in the cells. It rapidly and sharply increases to about 7 mA during the first days of the experiment and then continuously slowly increases up to about 8 mA after 3 weeks of exposure.

6.2. Aspect of the samples

When removing the sample exposed to 30 V and a CO$_2$ delivery set at either 100 mL/min every 10 min (Test 13) or at 100 mL/min every minute (Tests 11 and 14), similar observations can be made. The positive electrode appears as it did before exposure, whereas the cathode is covered by calcium carbonate. The sample at the anode side exhibits a slight calcium carbonate deposition on its most superficial part, and the cathode side of the sample exhibits a fragile behavior (occurrence of cracks) and has reacted with CO$_2$ over a thickness of few millimeters width to form calcium carbonate (Fig. 16).

6.3. Mineralogical evolution, microstructural characterization and front thickness

When analyzing the thick mineral precipitation at the cathode side of the sample, the common occurrence of calcite and vaterite is widely detected, and no portlandite remains preserved. At the anode side, only a low amount of calcium carbonate (calcite) is detected and portlandite is preserved.

Fig. 17 shows the sample cross sections highlighting the occurrence of a front for which the thickness varies with time and with the CO$_2$ flow and frequency of CO$_2$ bubbling in the cells. For fixed CO$_2$ delivery conditions, the alteration front visible at the cathode side penetrates the sample with time. Furthermore, for a fixed duration of exposure, when increasing the CO$_2$ flow and the frequency of bubbling, one can note that the thickness of

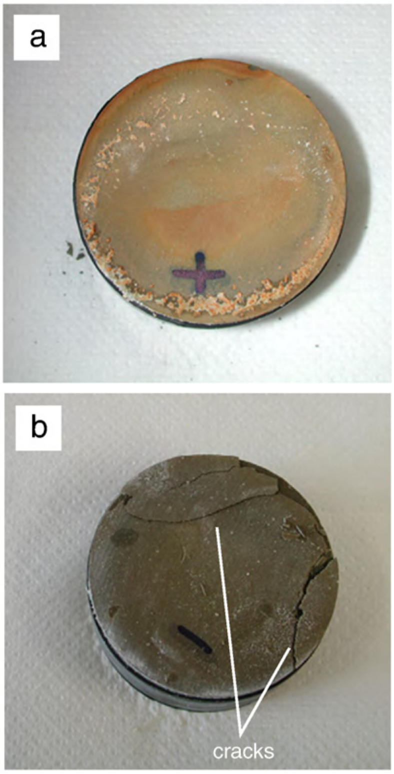

Fig. 16. Pictures of Portland cement sample at the anode side (a) and at the cathode side (b) for Test 14 (significant CO$_2$ delivery into the cells).

this front increases. For these tests at 30 V, when increasing the CO_2 flow and frequency of CO_2 bubbling in the cells (Tests 11, 13, and 14), SEM-BSE image analyses show that the alteration pattern at the cathode side consists of a dissolution zone and a diffuse carbonation/dissolution zone with opposite carbonation and dissolution gradients (Fig. 18), similar to the low CO_2 flow and less frequent bubbling (Tests 7 and 8). Furthermore, similar cracking is observed at the interface between the dissolution zone and the diffuse carbonation/dissolution zone, and radial cracks are also commonly observed within the dissolution zone. The thickness measurements of the different fronts are reported in Table 6, and the evolution of the alteration front thickness with time is plotted in Fig. 19. For a fixed duration, the increase of the CO_2 bubbling has an effect on the thickness of the diffuse carbonation/dissolution zone. It increases with the CO_2 flow and bubbling frequency (Table 6). In contrast, the thickness of the dissolution front remains constant (300 µm after 1 week and 700 µm after 3 weeks), whatever the CO_2 bubbling. After 3 weeks of exposure, no major difference is detected between the test with a bubbling frequency of 10 min (Test 13) and a nearly continuous bubbling (every 1 min; Test 14) (Table 6; Fig. 17). This may be related to the saturation of water by CO_2 that is completed at this test duration. Therefore, at this stage, any higher CO_2 delivery may not impact the acceleration rate of cement alteration.

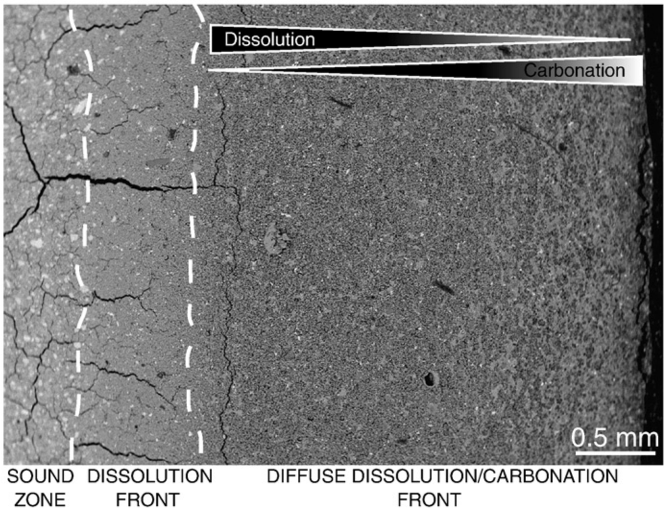

Fig. 18. SEM-BSE image showing the alteration pattern at the cathode side of a cement sample tested during 3 weeks at 30 V, and with a CO_2 delivery set at 100 mL/min every 10 min (Test 13).

6.4. Porosity evolution

Mercury intrusion porosimetry data are also reported in Table 6. The initial porosity of Portland cement, before exposure, is about 27.5%. After the test during 1 week, with a low CO_2 flow (25 mL/min, every 10 min), the porosity has increased and is about 31%. Afterwards, the porosity seems to be stable overtime (32% after 3 weeks). When comparing both durations of exposure, one can note that the dissolution front (having the effect of increasing the global porosity) thickness increases, as well as the carbonated zone (which may have the effect of plugging the porosity and thus decreasing the global porosity) thickness also increases. The two fronts may have opposite effects on the porosity evolution, which may explain the stability of the porosity over time. However, when comparing the two tests performed during 1 week, with a strong difference in the CO_2 flow into the electrolytes (25 mL/min. every 10 min vs. 100 mL/min every minute), one can notice that the porosity decreases. As reported in the table, the dissolution front thickness is the same for both tests (300 µm) whereas the diffuse zone thickness has increased (from 650 to 1200 µm), which may have the effect of decreasing the porosity. Nevertheless, this cannot be confirmed with the test during 3 weeks, since no data is available for the highest bubbling rate (100 mL/min every minute).

7. Conclusions

Portland cement exposed to a potential gradient alone (LIFT procedure) at atmospheric pressure and room temperature shows leaching due to the forced transport of the cement ionic species,

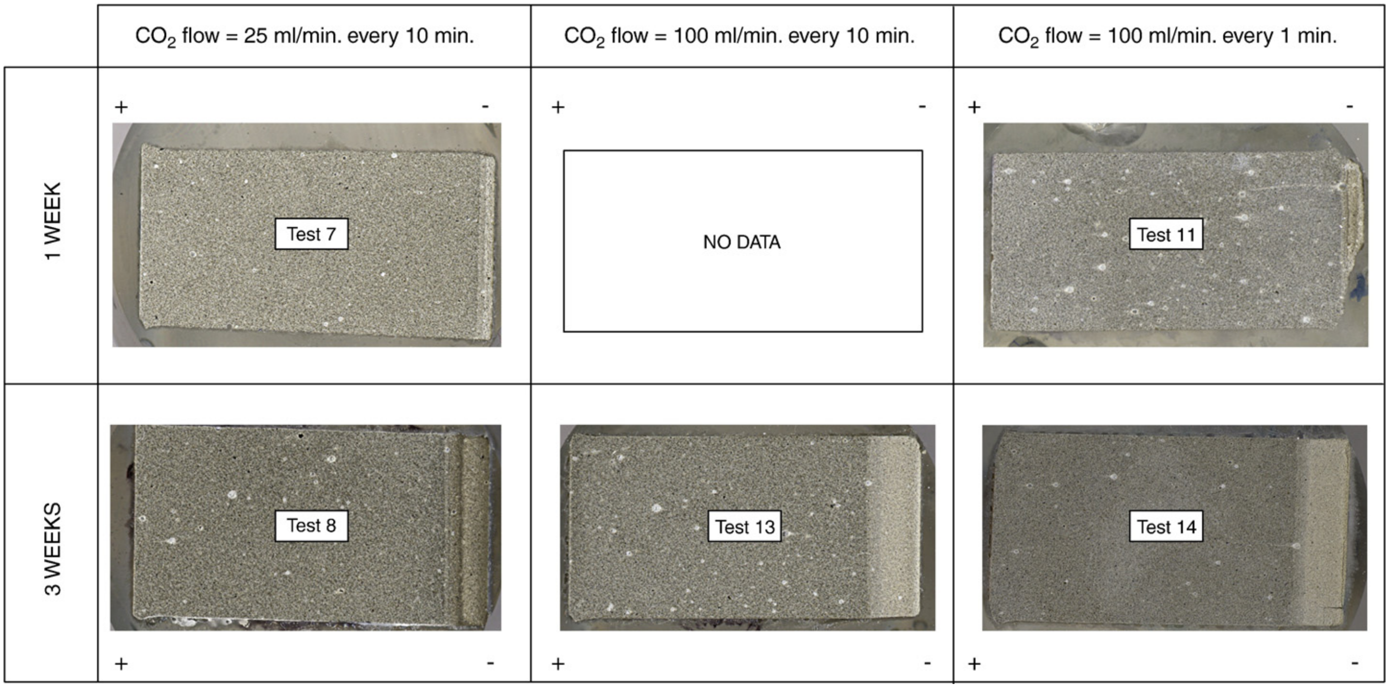

Fig. 17. Pictures of the sample cross-sections for Portland cement tested at 30 V, during one week and three weeks, with different conditions of CO_2 delivery in the electrolyte.

Table 6
Effect of the CO_2 bubbling delivery on the thickness of the different fronts in the altered zone at the cathode side and on the sample porosity. The thickness of the entire altered zone is also reported (alteration front = diffuse carbonation/dissolution zone + dissolution front).

Test name	Test conditions	Diffuse carbonation/ dissolution zone (μm)	Dissolution front (μm)	Alteration front (μm)	Sample porosity (%)
10	30 V, 1 week 25 mL/min $f = 10$ min	650	300	950	31
11	30 V, 1 week 100 mL/min $f = 1$ min	1200	300	1500	25.5
8	30 V, 3 weeks 25 mL/min $f = 10$ min	2100	700	2800	32
13	30 V, 3 weeks 100 mL/min $f = 10$ min	2900	700	3600	32
14	30 V, 3 weeks 100 mL/min $f = 1$ min	3000	700	3700	–

particularly towards the negative electrode (cathode). The leaching is restricted to a uniform alteration front in which portlandite is dissolved and the C–S–H phases are decalcified. Radial cracking is associated with the leaching of the cement ionic species. The kinetics of cement degradation is proportional to the time of exposure, the diffusion process being too slow to be considered.

Portland cement exposed to CO_2 bubbling alone (0 V) in the LIFTCO$_2$ vessel shows an alteration front visible at both edges of the samples. The alteration front pattern consists of a dissolution front, a carbonation front, and a gel layer, similar to the observations from previous studies in autoclaves under pressure and temperature [1]. The thickness of this alteration front is 10 times smaller than that at 280 bars and 90 °C. The slower kinetics of alteration is explained by the lower CO_2 solubility and lower cement permeability at atmospheric conditions and ambient temperature.

When applying a potential gradient through the cement in CO_2-rich environment (LIFTCO$_2$ procedure), it is possible to accelerate cement degradation. Indeed, the alteration front penetration at the cathode side is deeper with the application of a potential gradient than without. Furthermore, increasing the voltage amplifies the forced transport of the cement ionic species, enhancing the decalcification and dissolution of cement components. This results in the release of more ions in the electrolyte available to react with CO_2, and thus accelerates the penetration of the alteration front into the sample. Therefore, this method consisting in the application of a voltage through a cement sample in a CO_2-fluid is an accelerated degradation method that may be suitable for investigations on the behavior of cement in CO_2-rich environment. On one hand, similar types of experiments with CO_2 in a same kind of apparatus but operating under pressure may be useful to quantify the acceleration rates (most likely higher than at atmospheric pressure) in an environment in which CO_2 has a significantly higher solubility. On the other hand, it should be noted that further investigations may be required to demonstrate that the acceleration provided by the voltage does not involve a slight change in the reaction mechanism.

The CO_2-related alteration of cement is accelerated when increasing the temperature. Indeed, the alteration front thickness is greater at 40 °C than at 20 °C. The carbonated zone is particularly more diffuse at 40 °C than at 20 °C. An increase of temperature amplifies the forced transport of the cement ionic species. In other terms, it enhances the decalcification or dissolution of cement phases. More ionic species are released in the electrolyte and are available to react with CO_2 and to form a thicker alteration front. The effect of the lower solubility of CO_2 at 40 °C than at 20 °C on the acceleration of cement alteration is negligible compared to the strong impact of the ionic species diffusivity that is higher at 40 °C than at 20 °C.

Increasing the CO_2 flow and bubbling frequency in the cells increases the CO_2 concentration in the electrolytes. The amount of calcium carbonate that precipitates at the cathode side is high and the thickness of the alteration front is greater than for low CO_2 flow and low bubbling frequency. Cracking is commonly observed at the cathode side and is attributed to the combination of cement carbonation and leaching of the cement species related to the application of the voltage. For a fixed duration, the increase of the CO_2 bubbling has an effect on the thickness of the diffuse carbonation/dissolution zone, which increases, but not on the thickness of the dissolution front, which remains constant whatever the CO_2 bubbling. The effect of renewing the fluid on the alteration of cement in CO_2-rich environment while the transport is forced by the voltage would be useful to investigate. Finally, although this study shows that cement degradation is accelerated when increasing the potential gradient, the temperature, and the CO_2 concentration in the electrolyte, one has to note that there is no clear way to relate the effect of increased voltage to increased temperature, pressure, or CO_2 concentration.

Acknowledgements

The authors would like to thank the management of Schlumberger for permission to publish this paper. The laboratory staff of Schlumberger Riboud Product Center, especially Hafida Achtal and Bernard Dargaud, is especially acknowledged. Two anonymous

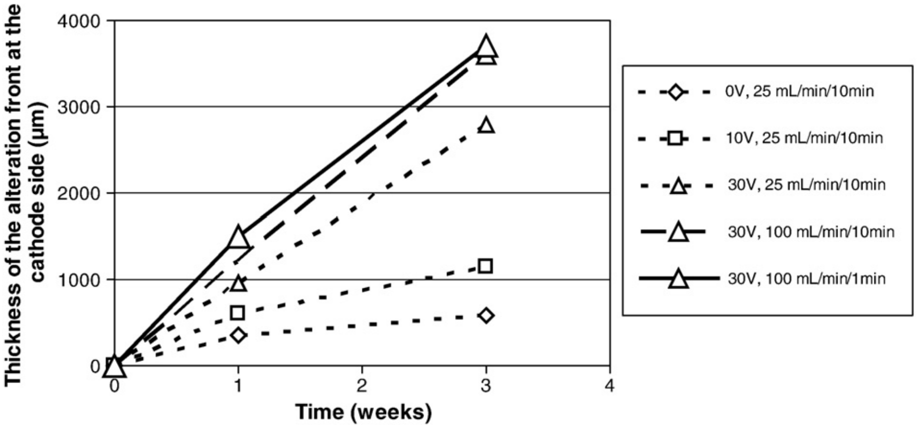

Fig. 19. Evolution of the alteration front thickness with time, for tests with varying potential gradient and varying CO_2 bubbling in the electrolytes.

reviewers are gratefully thanked for fruitful comments and suggestions which greatly improved the first version of the manuscript.

References

[1] V. Barlet-Gouédard, G. Rimmelé, B. Goffé, O. Porcherie, Mitigation strategies for the risk of CO_2 migration through wellbores, *IADC/SPE 98924*, Miami, USA, February 2006.

[2] V. Barlet-Gouédard, G. Rimmelé, B. Goffé, O. Porcherie, Well technologies for CO_2 geological storage: CO_2-resistant cement, oil and gas science and technology, Revue de l'Institut Francais du Petrole 62 (3) (2007) 1–12.

[3] G. Rimmelé, V. Barlet-Gouédard, O. Porcherie, B. Goffé, F. Brunet, Heterogeneous porosity distribution in Portland cement exposed to CO_2-rich fluids, Cement and Concrete Research 38 (2008) 1038–1048.

[4] B. Kutchko, B. Strazisar, D. Dzombak, G. Lowry, Degradation of well cements under geologic sequestration conditions, Wellbore Integrity network Meeting, Princeton, N.J, March 29, , 2006.

[5] B. Kutchko, B. Strazisar, D. Dzombak, G. Lowry, N. Thaulow, Degradation of well cement by CO_2 under geologic sequestration conditions, Environmental Science and Technology 41 (2007) 4787–4792.

[6] A. Duguid, M. Radonjic, G. Scherer, The effect of carbonated brine on the interface between well cement and geologic formations under diffusion-controlled conditions, 8th International conference on Greenhouse Gas Control Technologies, Trondheim, Norway, June 19–22 2006.

[7] N. Jacquemet, J. Pironon, E. Caroli, A new experimental procedure for simulation of $H_2S + CO_2$ geological storage — application to well cement aging, Oil and Gas Science and Technology – Rev IFP 60 (1) (2005) 93–206.

[8] Jacquemet, N. (2006). Durabilité des matériaux de puits pétroliers dans le cadre d'une séquestration géologique de dioxyde de carbone et d'hydrogene sulfuré, PhD thesis, Université H. Poincaré, Nancy I.

[9] J.W. Carey, M. Wigand, S. Chipera, et al., Analysis and performance of oil well cement with 30 years of CO_2 exposure from the SACROC unit, West Texas, USA, 8th International conference on Greenhouse Gas Control Technologies, Trondheim, Norway, June 19–22 2006.

[10] J.W. Carey, M. Wigand, S. Chipera, et al., Analysis and performance of oil well cement with 30 years of CO_2 exposure from the SACROC unit, West Texas, USA, International Journal of Greenhouse Gas Control (2007) 75–85. doi:10.1016/S1750-5836(06)00004-1.

[11] H. Saito, S. Nakane, S. Ikari, A. Fujiwara, Preliminary experimental study on the deterioration of cementitious materials by an acceleration method, Nuclear Engineering and Design 138 (1992) 151–155.

[12] H. Saito, A. Deguchi, Leaching tests on different mortars using accelerated electrochemical method, Cement and Concrete Research 30 (11) (2000) 1815–1825.

[13] B. Gérard (1996). Contribution des couplages mécanique-chimie-transfert dans le long terme des ouvrages de stockages de déchets radioactifs. Thèse de doctorat; LMT-ENS Cachan et Université de Laval (Québec).

[14] N. Spycher, K. Pruess, CO_2–H_2O mixtures in the geological sequestration of CO2. II. Partitioning in chloride brines at 12–100 °C and up to 600 bar, Geochimica et Cosmochimica Acta 69 (13) (2005) 3309–3320.

[15] N. Spycher, K. Pruess, J. Ennis-King, CO_2-H_2O mixtures in the geological sequestration of CO_2. I. Assessment and calculation of mutual solubilities from 12 to 100 °C and up to 600 bar, Geochimica et Cosmochimica Acta 67 (16) (2003) 3015–3031.

[16] Portier, S. (2005). Solubilité de CO_2 dans les saumures des basins sédimentaires. Application au stockage de CO_2 (gaz a effet de serre). Ph.D thesis, Université Louis Pasteur, Strasbourg I.

[17] S. Portier, C. Rochelle, Modelling CO_2 solubility in pure water and NaCl-type waters from 0 to 300 8C and from 1 to 300 bar. Application to the Utsira Formation at Sleipner, Chemical Geology 217 (2005) 187–199.